# Gap solitons in anharmonic one-dimensional asymmetrical physical systems with Kac-Baker long-range interactions

C. Tatuam Kamga[1] and T. C. Kofane[2]

[1]*Laboratoire de Physique de l'Université de Bourgogne, Phénomènes Non Linéaires: Faculté des Sciences et Techniques, 6 boulevard Gabriel, 21000 Dijon, France*

[2]*Laboratoire de Mécanique, Faculté des Sciences, Université de Yaoundé I, Bôite Postale 812 Yaoundé, Cameroon*

(Received 28 March 1994)

We present an analytical and numerical study of the nonlinear response near the lower gap of a simple system that is intercalated between two linear systems. In this finite system, the long-range interaction potential of the Kac-Baker type is taken into account in addition to the nonlinear substrate potential, which is naturally asymmetrical or has its symmetry broken by an external force. The modulated wave solutions are investigated in the weakly nonlinear case and in the small wave vector limit to calculate the gap soliton envelope and the transmissivity that presents bistability. The results in connection with the sine-Gordon system are discussed. It is shown that when the long-range interaction parameter increases, the bistability of the system tends to disappear in the cooperative short-range interactions case. Also in the competitive short-range interaction case, there are hole gap standing waves for larger values of the long-range parameter.

PACS number(s): 42.25.Bs, 42.65.Pc, 78.20.Dj

## I. INTRODUCTION

The nonlinear response and transmission properties of one-dimensional systems such as periodic structures [1,2], nonabsorbing [3–5] and absorbing [6,7] superlattices, and quasiperiodic [8] structures of finite dimension have been extensively studied. More recently again, the transmission properties of one-dimensional systems perturbed by an external constant force and submitted to any substrate potential (symmetrical or asymmetrical) [9] have been studied. The infatuation for this branch of nonlinear physics comes from the large range of physical applications that are related to it. One can note, for example, the transmission through optical fibers that occurs with great incidence in optical communications, the memory effects of certain lattices resulting from their multistability, and finally the possibility of forcing the intimate characteristics of some materials by compelling them to propagate and transmit waves that they naturally impede. Most of the works previously mentioned have been focused on optical systems and thereby do not present any general aspect as to their application in other scopes of physics. By contrast, other more general works are based on the intimate structure of the lattice via the motion of its particles and can be reset by analogy with optical models. However, many studies of the lattice vibrations in one-dimensional chains of atoms have been based essentially on short-range interactions. For example, the Frenkel-Kontorova model of dislocation dynamics [10] is a simple model of a chain of atoms interacting via next neighbor harmonic forces and placed in a periodic external substrate potential. The Toda lattice [11], which is an atomic linear chain with exponential nearest neighbor forces, has been refined and extended to treat real physical systems where interatomic forces extend further than the nearest neighbors. Thus the various types of long-range interatomic forces commonly encountered are the power-law interactions [12,13], the Lennard-Jones long-range coupling [14], and the Kac-Baker long-range interaction [15,16]. The power-law interaction models have been found to yield improved quantitative agreement with some experimental features such as the explanation of the observed finite exponent that appears on the density of solitons at zero temperature [12]. In the case of lattice models with a long-range coupling of the Lennard-Jones type, it has been shown that the value of the long-range parameter does not contribute to the nonlinear term but to the dispersion terms of the equation of propagation in the continuum limit [14]. The Kac-Baker long-range interaction is a well studied example in which the interactions between particles fall off exponentially as the distance between them increases. It has been used by many authors to analyze the thermodynamics of systems such as the Ising [15,16], Pott [17], continuum $\Phi^4$ [18], as well as the discrete $\Phi^4$ models [19–21]. It has also been used to study the effect of long-range interactions on the properties of the nontopological solitonlike excitations in one-dimensional anharmonic monatomic [22] and diatomic [23] lattices in a compressible Heisenberg chain [24], on the topological solitons in the sine-Gordon system [25], and on the classical statistical mechanics of one-dimensional sine-Gordon and double sine-Gordon systems [26,27]. The energetic analysis has been used to study the effect of a perturbing force on the Kink motion in a $\Phi^4$ system with the Kac-Baker potential. It has been shown that the kink velocity or mobility not only depend on the external field, but also on the long-range interaction parameter [28]. Another interesting result is that the intensity of the central peak decreases, whereas peaks of the soft-phonon mode increase [29]. One fundamental aspect of the long-range interactions was pointed out by Remoissenet and Flytzanis,

 

who showed the possible coexistence of supersonic and subsonic kink pulse solitons found in the continuum approximation, and the existence of a domain velocity separated by gaps whose width can be modulated by the long-range parameter [22]. They also show that in the low amplitude limit of oscillations, envelope and dark solitons can coexist in a continuous chain allowing, moreover, anharmonic cubic interactions between nearest neighbors [22]. However, it follows from this glimpse that, as far as we know, no study has focused on finite lattices allowing long-range interactions. In addition, no attention has been paid to the transmission properties of such systems, perturbed by an external constant force and admitting harmonic and anharmonic interactions between nearest neighbors. In the continuum limit approximation and considering the Kac-Baker long-range coupling, we will base our investigations on this topic. Thus there is considerable interest in understanding and improving nonlinear responses of finite systems admitting long-range interactions, both from a theoretical viewpoint as well as from the viewpoint of experimentalists, who need such models to explain features in real physical systems. Our paper is organized as follows. In Sec. II, we present the general discrete model and its continuum approximation. After looking for the envelope function equation in the low-amplitude limit in Sec. III, boundary conditions are found in Sec. IV and stationary solutions are presented in Sec. V. Numerical discussions and concluding remarks are presented in Sec. VI to outline the principal points of our investigations.

## II. MODEL

The system considered is a perfect one-dimensional (1D) nonlinear monatomic lattice intercalated between two linear 1D lattices. Along the $x$ direction, an incident wave with angular frequency $\omega$, scalar dimensionless field amplitude $E_0$, and wave number $k_L=\omega/c_L$ propagating in a linear medium (1) with velocity $c_L$ strikes at $x=0$, a nonlinear medium (2) of length $L$ with discrete masses $m$. The nonlinear and linear lattice steps are, respectively, $a$ and $b$. The quantity $R$ is the amplitude of the reflected wave measured with respect to $E_0$ and $T$ is the amplitude of the transmitted wave at $x=L$ in the linear medium (3). Within the nonlinear medium, each particle interacts with its nearest neighbors through a potential that includes a cubic and quartic nonlinearity. Moreover, each particle $i$ interacts with another particle $j$, inducing long-range interactions. We assume that the field $y_i(t)$ obeys the Hamiltonian of the form

$$H=\tfrac{1}{2}\sum_i m\left[\frac{dy_i}{dt}\right]^2+\sum_i U(y_i)+\sum_i \omega_0^2 V(y_i)+\sum_{i\neq j}\tfrac{1}{2}V_{ij}(y_i-y_j)^2 . \tag{2.1}$$

The first term of the right hand side of Eq. (2.1) represents the kinetic energy carried by the field; the second term is the nonlinear short-range potential that describes harmonic and anharmonic interactions between nearest neighbors. It takes the form

$$\sum_i U(y_i)=\sum_i\left[\tfrac{1}{2}k_2(y_i-y_{i-1})^2+\tfrac{1}{3}k_3(y_i-y_{i-1})^3+\tfrac{1}{4}k_4(y_i-y_{i-1})^4\right] , \tag{2.2}$$

where $k_2$, $k_3$, and $k_4$ are harmonic, cubic, and quartic anharmonic interaction coefficients, respectively. The third term is the symmetrical (sine-Gordon) or asymmetrical ($\Phi^4$) substrate potential. The last term in the Hamiltonian is a harmonic Kac-Baker long-range pair potential [18,22]:

$$V_{ij}=\left[\frac{J(1-r)}{2r}\right]r^{|i-j|} . \tag{2.3}$$

The coefficient $J$ is a constant measuring the elastic energy of the lattice and $r$ is a parameter that characterizes the intensity of the long-range interactions. The limiting values of $r$ are such that $0\le r\le 1$; the absolute difference $|i-j|$ measures the distance between sites $i$ and $j$. The virtue of this interaction potential is that the range can vary continuously. The interaction between particles falls off exponentially as the separation between them increases. The prefactor $(1-r)$ in Eq. (2.3) is chosen to ensure that the total potential experienced by one atom, due to all others, is finite in the thermodynamic limit [18,22,20]. Thus we have

$$\sum_{i\neq y} V_{ij}=J . \tag{2.4}$$

In a finite system, the number of particles is finite and (2.4) is valid only in a certain limit $r_c$ of the parameter $r$, as we will show in our numerical results. Consequently, $J$ is independent of the range of interactions. The equation of motion of the $i$th particle derived from (2.1) is

$$\begin{aligned} m\frac{d^2y_i}{dt^2}=&k_2(y_{i+1}-2y_i+y_{i-1})\\ &+k_3[(y_{i+1}-y_i)^2-(y_i-y_{i-1})^2]\\ &+k_4[(y_{i+1}-y_i)^3-(y_i-y_{i-1})^3]-G_0^2\frac{dV(y_i)}{dy_i}\\ &-J\left[\frac{1-r}{r}\right]\sum_{i\neq j} r^{|i-j|}(y_i-y_j) . \end{aligned} \tag{2.5}$$

Afterwards, we will put $J_p=J/m$, $G_i=k_i/m$ $(i=2,3,4)$, and $\omega_0^2=G_0^2/m$. With these definitions, and using Eq. (2.4), we rewrite Eq. (2.5) in the reduced form,

$$\frac{d^2y_i}{dt^2}=\mathcal{F}_i-\omega_0^2\frac{dV(y_i)}{dy_i}-2J_p y_i+L_i , \tag{2.6}$$

where $\mathcal{F}_i$ is the harmonic, cubic, and quartic anharmonic interaction forces between nearest neighbors corresponding to the first three terms of the right hand side of Eq. (2.5). The auxiliary quantity $L_i$ is given by

$$L_i=\frac{J_p(1-r)}{r}\sum_{i\neq j} r^{|i-j|}y_j . \tag{2.7}$$

Introducing the quantities $L_{i+1}$ and $L_{i-1}$ we get the following recursive relation:

$$\left[r+\frac{1}{r}\right]L_i=(L_{i+1}+L_{i-1})+\frac{J_p(1-r)}{r}(y_{i+1}-2ry_i+y_{i-1}), \quad (2.8)$$

which only implies nearest neighbor terms. This property is going to be very useful to obtain the discrete motion equation. We now make the continuum approximation, which assumes that the lattice is excited by waves of great spatial extension. This implies a slow variation of the surface wave curvature during its spatiotemporal variation. Consequently, terms in Eqs. (2.8) and (2.5) implying subscripts $i+1$ and $i-1$ can be expanded in a Taylor series up to the four order derivatives. This increases the dispersion and allow us to balance the nonlinearity introduced by anharmonic interactions. Therefore, the resulting equation of motion in the continuum approximation is

$$y_{tt}-\chi_0 y_{xx}+\omega_0^2\frac{dV}{dy}=\chi_1 y_{ttxx}+\chi_2 y_{xxxx}+p[(y_x)^2]_x+q[(y_x)^3]_x+\chi_3\left[a^2\left[\frac{dV}{dy}\right]_{xx}+\frac{a^4}{12}\left[\frac{dV}{dy}\right]_{xxxx}\right], \quad (2.9)$$

where the subscripts denote partial derivatives according to the corresponding variables. Coefficients of Eq. (2.9) are defined by

$$\chi_0=a^2\left[G_2+\frac{J_p(1+r)}{(1-r)^2}\right],\quad \chi_1=\frac{a^2 r}{(1-r)^2},$$
$$p=a^3G_3,\quad q=a^4G_4, \quad (2.10)$$
$$\chi_2=\frac{a^4}{12}\left[G_2+\frac{J_p(1+r)}{(1-r)^2}\right]-\frac{a^4 r}{(1-r)^2},$$
$$\chi_3=\frac{r\omega_0^2}{(1-r)^2}, \quad (2.11)$$

where the length scale $a$ is the step of the lattice. Some of these results were obtained [22] in the case of pure anharmonic chains (i.e., without any substrate potential). Looking for small oscillations near the bottom of the potential well, we write

$$y(x,t)=\phi_0+\epsilon\Phi(x,t), \quad (2.12)$$

where $\phi_0$ is the equilibrium position around which oscillations take place. For $\phi_0\neq 0$ the system is asymmetrical [30,9] ($\Phi^4$ potential) or symmetrical but perturbed by an external force (e.g., perturbed sine-Gordon system). The parameter $\epsilon$ is small so as to ensure collective oscillations $\Phi$ around $\phi_0$. Using Eq. (2.12), the derivatives of the substrate potential are expanded in terms of $\Phi$. Substituting the result in Eq. (2.9) yields

$$\Phi_{tt}-c^2(r)\Phi_{xx}+\omega_0'^2(\Phi+\epsilon\alpha\Phi^2+\epsilon^2\beta\Phi^3)=f(r)\Phi_{ttxx}+h(r)\Phi_{xxxx}+\epsilon[p(\Phi_x)^2]_x+\epsilon^2[q(\Phi_x)^3]_x+\epsilon s_0\left[(\Phi^2)_{xx}+\frac{a^2}{12}(\Phi^2)_{xxxx}\right]+\epsilon^2 s_1\left[(\Phi^3)_{xx}+\frac{a^2}{12}(\Phi^3)_{xxxx}\right], \quad (2.13)$$

where $\alpha=a_2/a_1$ and $\beta=a_3/a_1$ depend on the equilibrium position of oscillations that can be modified by an external force. Constants $a_1$, $a_2$, and $a_3$ are given by

$$a_k=\frac{1}{k!}\left[\frac{d^{k+1}V(\Phi)}{d\Phi^{k+1}}\right]_{\Phi=\phi_0},\quad k=1,2,3 \quad (2.14)$$

$$\omega_0'^2=a_1\omega_0^2,\quad c^2(r)=a^2\left[G_2+\frac{J_p(1+r)+r\omega_0'^2}{(1-r)^2}\right], \quad (2.15)$$

$$h(r)=\frac{a^4}{12}\left[G_2+\frac{J_p(1+r)+r\omega_0'^2}{(1-r)^2}\right]-\frac{ra^4G_2}{(1-r^2)}, \quad (2.16)$$

$$s_0=\alpha\frac{ra^2\omega_0'^2}{(1-r)^2},\quad s_1=\beta\frac{ra^2\omega_0'^2}{(1-r)^2}. \quad (2.17)$$

$c(r)$ is the velocity of linear waves. $f(r)=\chi_1$ and $h(r)$ are the dispersion coefficients; $s_0$ and $s_1$ are the nonlinear-dispersive coefficients relative to the substrate potential; $p$ and $q$ are nonlinear coefficients relative to the anharmonic cubic and quartic interactions, respectively. The characteristic velocity $c(r)$ and the dispersion coefficients $h(r)$ depend on the nature (symmetrical or asymmetrical) of the potential. Consequently, they can be modified by an external force, except for the case of no long-range interaction ($r=0$).

## III. ENVELOPE FUNCTION EQUATION

The general equation (2.13) obtained previously can lead to two main types of solutions usually encountered in nonlinear physics: pulse, kink soliton excitations and the solution of the nonlinear Schrödinger (NLS) equation, which is essentially valid in the weakly nonlinear case. Thus we will restrict ourselves to the weakly nonlinear case. It is well known that the NLS equation obtained from this approximation gives rise to two types of localized solutions in a medium infinitely extended. For a finite medium, standing waves are expected and the transmissivity can be characterized. Our main purpose is now to see how the transmissivity of the system can be controlled by the long-range interaction intensity. First of all, let us find the envelope nonlinear equation of the modulation. One way to determine the NLS equation is to derive the nonlinear dispersion relation and to apply the inverse Fourier transformation to the equation resulting from the Taylor expansion of the frequency around that of the carrier wave. For convenience, we use the

multiple scales method, where $x$ and $t$ are scaled into independent variables $x_0, x_1, \ldots, x_n$ and $t_0, t_1, \ldots, t_n$, respectively, with

$$x_n = \epsilon^n x, \quad t_n = \epsilon^n t \ . \tag{3.1}$$

The partial derivative operators can thus be written as

$$\frac{\partial}{\partial x} = \sum_{n=0}^{N} \epsilon^n \frac{\partial}{\partial x_n} \ , \tag{3.2}$$

$$\frac{\partial}{\partial t} = \sum_{n=0}^{N} \epsilon^n \frac{\partial}{\partial t_n} \ . \tag{3.3}$$

We now transform Eq. (2.13) by assuming the expansion until the second harmonic generation. Thus we can write the solution in terms of the envelope continuum component $F_0(x,t)$, and envelopes of the first and second harmonics, respectively, $F_1(x_1,t_1)$ and $F_2(x_1,t_1)$; we get [33,34]

$$\Phi = [F_1(x_1,t_1)e^{i(k_p x_0 - \omega_p t_0)} + \text{c.c.}] + \epsilon[F_0 + F_2(x_1,t_1)e^{2i(k_p x_0 - \omega_p t_0)} + \text{c.c.}] \ , \tag{3.4}$$

where c.c. represents the complex conjugate, and the variables $k_p$ and $\omega_p$ represent the wave number and angular frequency of the carrier wave, respectively. We now substitute Eqs. (3.1)–(3.4) in Eq. (2.13). Collecting constant terms yields, after some simplifications, the linear dispersion relation

$$\omega_p^2 = \frac{\omega_0'^2 + k_p^2 c^2(r) - k_p^4 h(r)}{1 + f(r)k_p^2} \ . \tag{3.5}$$

The shapes of the linear dispersion curve are shown in Figs. 1(a) and 1(b). We note that in both cases (cooperative and competitive short-range interactions) there is a linear natural gap whose threshold is at $\omega_p = 1.0$ for $\phi_0 = 0.0$. This natural gap comes from the substrate potential considered in the model. For each of the short-range interactions, the wave's dispersion in the nonlinear medium increases with the long-range parameter $r$. For greatest values of the parameter $r$, and in particular for $r = 0.9$, we note that in the competitive short-range interactions the threshold of the gap changes; it is at $\omega = 0.9346$ instead of $\omega = 1.0$. Consequently, for $J_p = -0.1$, $r = 0.9$, and $\omega_0 = 0$ (no substrate potential), the linear dispersion curve is undefined for low wave numbers ($k_p < 0.44$). In fact, in this range of wave number values, the angular frequency is negative. This unphysical behavior of the linear dispersion arises when one attempts to consider values of $r$ greater than the critical long-range parameter $r_c$ for a given negative value of $J_p$. For $J_p \geq 0$ or $\omega_0 = 0$, this critical value $r_c$ does not exist. Expression (3.5) is equivalent to that obtained previously [22] for $\omega_0' = 0$, which is the lower gap edge of the dispersion curve. In our case, the lower gap edge varies with the deformation of the substrate potential submitted to external perturbations. Those perturbations are assumed to be constant in space and time.

Collecting the first-order terms [i.e., $O(\varepsilon)$] of the zero and second harmonic, one gets, respectively,

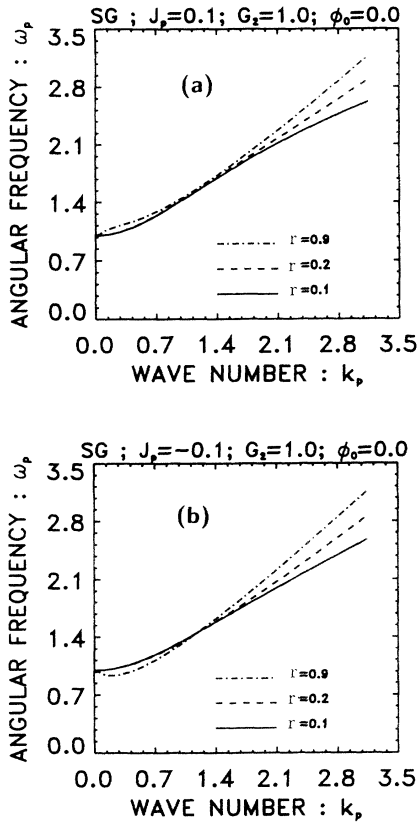


FIG. 1. Linear dispersion curves for the symmetrical sine-Gordon system ($\phi_0 = 0$): (a) the cooperative short-range interactions ($J_p > 0$ and $G_2 > 0$), and (b) the competitive short-range interactions ($J_p < 0$ and $G_2 > 0$).

$$F_0 = -2\alpha |F_1|^2 \tag{3.6}$$

and

$$F_2 = \mu_{0r} F_1^2 \ . \tag{3.7}$$

$F_2$ is obtained by assuming $p = 0$ (for simplification). Physically, the coefficient $p$ increases the nonlinearity; this is not especially needed since we are restricted to the weakly nonlinear case. The coefficient appearing in (3.7) is given by

$$\mu_{0r} = \frac{[1 + k_p^2 f(r)][4k_p^2 s_0(3 - a^2 k_p^2) + 3\alpha\omega_0'^2]}{9[\omega_0'^2(1 + 5k_p^2 f(r)) + 4k_p^4(h(r) + c^2(r)f(r))]} \ . \tag{3.8}$$

We now collect second order terms of the second harmonic, and we set

$$\zeta = x_1 - v_g t_1, \quad \tau = \epsilon t_1 \ . \tag{3.9}$$

Using (3.6) and (3.7), we get

$$i\frac{\partial F_1}{\partial \tau} + P\frac{\partial^2 F_1}{\partial \zeta^2} + Q|F_1|^2 F_1 = 0 \ , \tag{3.10}$$

where $P$ is the group-velocity dispersion given by

$$P=-\frac{[1+k_p^2f(r)]v_g^2+\omega_p^2f(r)+6k_p^2h(r)-c^2(r)+4k_p\omega_pf(r)v_g}{2\omega_p[1+k_p^2f(r)]}\ , \tag{3.11}$$

with $v_g$ the group velocity expressed as

$$v_g=\frac{k_p[c^2(r)-\omega_p^2f(r)-2k_p^2h(r)]}{\omega_p[1+k_p^2f(r)]}\ . \tag{3.12}$$

For the incoming wave angular frequency near the lower gap edge whose frequency is $\omega_p$, we have $(k_p,\omega_p)=(0,\omega_0')$ and, therefore, $v_g=0$. The nonlinear coefficient $Q$ in (3.10) is given by

$$Q=-\frac{k_p^2[(\mu_{0r}-2\alpha)(2-\frac{1}{6}a^2k_p^2)s_0+(3-\frac{1}{4}a^2k_p^2)s_1+3k_p^2q]+\omega_0'^2(3\beta+2\alpha\mu_{0r}-4\alpha^2)}{2\omega_p[1+k_p^2f(r)]}\ . \tag{3.13}$$

We now study the sign of $K=PQ$; this allows us to know what type of low-amplitude solution is expected in the nonlinear medium, recalling that for $K>0$ and $K<0$, envelope and hole solutions are respectively expected. Looking for the region of the long-range parameter in which one could have each type of solution (envelope or dark solution), we study in Fig. 2 the behavior of $PQ$ as a function of $r$ in the competitive short-range interactions. We note that when $|J_p|$ increases, the region of the long-range parameter $r$ in which one could expect a hole solution is stretched. In the case of cooperative interactions, we easily note that only envelope solutions exist. The main difference with the Remoissenet-Flytzanis case is the presence of the substrate potential and the quartic nonlinear interactions between first neighbors. Equation (3.10) is the NLS equation, which will be the starting point of the derivation of the standing wave equation.

## IV. BOUNDARY CONDITIONS

Our purpose is to find the boundary conditions between linear and nonlinear media implying long-range interactions. The starting point is Eq. (2.13), which describes the collective oscillations in the nonlinear medium. Because the envelope function does not mainly depend on the nonlinearity close to the rear of the nonlinear medium, nonlinear terms are neglected in the equation of motion. The remaining equation evolves fourth-order derivatives in terms of variables $x$ and $t$:

$$\Phi_{tt}-c^2(r)\Phi_{xx}+\omega_0'^2\Phi=f(r)\Phi_{ttxx}+h(r)\Phi_{xxxx}\ . \tag{4.1}$$

Because of the presence of these higher-order partial derivatives greater care must be taken when searching analytic expressions for the matching conditions. Equation (2.13) can in fact be obtained by writing the total energy conservation. The conservation of energy flow can thus be deduced. The straightforward procedure is first to write the finite difference representation of each partial derivative relative to variable $x$. Second, each term of the finite difference is expanded in a Taylor's series. For a stationary monochromatic incoming wave of frequency $\omega$, the operator $\partial/\partial t$ is substituted by $-i\omega$. Finally, we assume that there is no long-range and short-range interaction (respectively, $r=0$ and $J_p=0$) in the linear systems. Thus in the resulting equation of motion, we have $c(r)=c_L$, $f(r)=0$, and $h(r)=h_0$, where $h_0=c_L^2a^2/12$. The nonzero value of $h_0$ comes from the expansion in a Taylor's series up to order 4 by applying the continuum medium approximation to discrete linear media. The conservation of energy flow at $x=0$ is then

$$\left[\frac{\partial\Phi_2}{\partial x}\right](0,t)=\mu_1\left[\frac{\partial\Phi_1}{\partial x}\right](0,t)-\mu_2\Phi_2(0,t)\ , \tag{4.2}$$

where the subscripts 1 and 2 on $\Phi$ are relative to the linear and nonlinear media, respectively. Constants $\mu_1$ and $\mu_2$ are given by

$$\mu_1=\frac{a^2c_L^2-2h_0}{a^2[c^2(r)-\omega^2f(r)]-2h(r)} \tag{4.3}$$

and

$$\mu_2=\frac{a^2[\omega^2-\omega_0'^2]}{a^2[c^2(r)-\omega^2f(r)]-2h(r)}\ . \tag{4.4}$$

In the same way, the conservation of energy flow at $x=L$ is given by

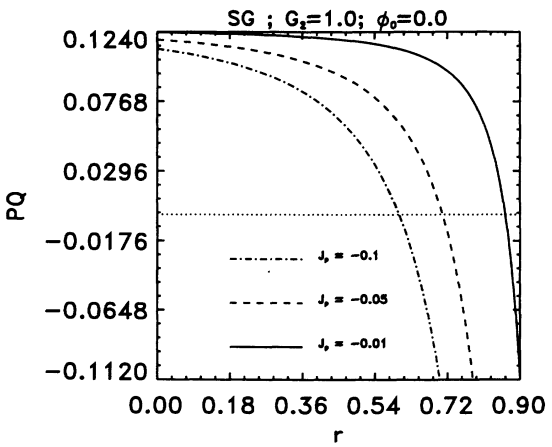


FIG. 2. Behavior of the characteristic dispersive-nonlinear coefficient $K=PQ$ as a function of the long-range parameter and for different values of $J_p$. The unperturbed sine-Gordon system allowing competitive short-range interactions is considered ($\phi_0=0$). When $PQ$ is negative, dark type solutions are expected. The corresponding region of $r$ depends on the value of the short-range parameter $J_p$. $PQ$ and $r$ are dimensionless.

$$\left[\frac{\partial\Phi_2}{\partial x}\right](L,t)=\mu_1\left[\frac{\partial\Phi_3}{\partial x}\right](L,t)+\mu_2\Phi_2(L,t)\ , \tag{4.5}$$

where the subscript 3 refers to the linear medium at the output of the nonlinear medium. The continuity of the wave amplitude at the boundaries is given by

$$\Phi_1(0,t)=\Phi_2(0,t)\ , \tag{4.6}$$

$$\Phi_2(L,t)=\Phi_3(L,t)\ . \tag{4.7}$$

Limiting ourselves to the first harmonic term, we write

$$\Phi_1(x,t)=E_0(e^{ik_Lx}+Re^{-ik_Lx})e^{-i\omega t} \quad \text{for } x\le 0\ , \tag{4.8}$$

$$\Phi_2(x,t)=E_0[q(x)e^{i\sigma(x)}e^{ik_px}]e^{-i\omega t} \quad \text{for } 0\le x\le L\ , \tag{4.9}$$

$$\Phi_3(x,t)=E_0Te^{ik_Lx}e^{-i\omega t} \quad \text{for } x\ge L\ , \tag{4.10}$$

where $q(x)$ and $\sigma(x)$ are, respectively, the spatial slowly varying amplitude and the phase of the envelope function; insertion of (4.9) and (4.10) in (4.7) yields $|T|=q(L)$. This means that the amplitude of the envelope function at the output of the nonlinear medium corresponds to the transmissivity of the system. As $|T|\le 1$, we should always have $q(L)\le 1$. This will be useful in our numerical studies. Inserting Eqs. (4.6)–(4.10) in (4.2) and (4.5) yields, after some simplifications, the following results:

$$\left[2\mu_2I_0+\left[\frac{dI}{dx}\right]_0\right]^2+4\mu_1^2k_L^2I_0^2\left[\frac{I_L}{I_0}+1\right]^2=16\mu_1^2k_L^2I_0\ , \tag{4.11}$$

where $I=q^2(x)$ is the intensity of the envelope function; $I_L$ and $I_0$ are, respectively, the envelope intensities at $x=0$ and $x=L$. Equation (4.11) is the boundary condition at $x=0$. Near the lower gap of the system, we have $\omega\simeq\omega_0'$ and consequently $\mu_2\simeq 0$. The boundary condition at the input of the nonlinear medium is then

$$\left[\left[\frac{dI}{dx}\right]_0\right]^2+4\mu_1^2k_L^2I_0^2\left[\frac{I_L}{I_0}+1\right]^2=16\mu_1^2k_L^2I_0\ . \tag{4.12}$$

Note that for $h_0=0$, $r=0$, $J_p=0$, $h(r)=f(r)=0$, and $c^2(r)=c_0^2$, we recover the previous results [9].

## V. STATIONARY SOLUTIONS OF THE NONLINEAR SCHRÖDINGER EQUATION

The NLS equation obtained previously governs the modulation of a quasimonochromatic wave train in the case of weakly nonlinear and dispersive systems. This equation yields to well-known applications in optics, plasma physics, and fluid dynamics. The particular interest of this equation is its complete integrability. Under certain boundary conditions that decay as $x\to\pm\infty$, it has been shown that the NLS equation admits soliton solutions. When the nonlinear medium is bounded (i.e., $0\le x\le L$), solutions are expressed in terms of Jacobian elliptic functions [2]. In this case, the envelope function is at rest in the space because of the vanishing of the group velocity; from expressions (3.12), it follows that $v_g=0$ for $k_p=0$, implying that the carrier wave vector is at the middle of the Brillouin zone and thus no energy is transported. Therefore, the NLS equation (3.10) depends only on space and time variables $x$ and $t$, respectively. Let us consider the transformation

$$F_1(x,t)=E(x)e^{-i\Omega t}\ , \tag{5.1}$$

where $\Omega$ is the envelope angular frequency defined by

$$\Omega=\omega-\omega_p\ , \tag{5.2}$$

with $\omega_p$ the carrier wave frequency and $\omega$ that of the incoming wave striking the nonlinear medium. To assume the slow variations of the envelope function, $\Omega$ must be neglected compared to $\omega_p$ and $\omega$ (i.e., $\Omega\ll\omega_p\simeq\omega$). $E(x)$ gives the spatial shape of the envelope function. Substituting (5.1) in the NLS equation, one obtains

$$\frac{d^2E}{dx^2}+\frac{\Omega}{P}n^2(|E|)E=0\ , \tag{5.3}$$

which is the Helmholtz equation relative to a homogeneous nonlinear system. The variable $n(|E|)$ is the optical analog of the index of refraction; it depends on $|E|$ via the relation

$$n^2(|E|)=1+\frac{Q}{\Omega}|E|^2\ . \tag{5.4}$$

The dependence of $n(|E|)$ on the amplitude function $|E|$ shows the compatibility of Eq. (5.3) with the nonlinearity of the system: the well-known nonlinear Kerr effect. In the case of inhomogeneous nonlinear systems, it is usual to add on the right hand side of (5.4) a function $\mu(x)$ that describes the distribution of impurities. This is particularly the case of random media [31]. $(\Omega/P)^{1/2}$ contained in (5.3) is the wave number of the linear waves in the medium. We note that for opposite signs of $\Omega$ and $P$ ($\Omega\le 0$ and $P\ge 0$), the incoming wave frequency lies in the natural gap of the continuous system. The knowledge of the function $E(x)$ suffices to give the properties of the envelope function in the nonlinear medium. Let us find the solution of (5.3) in the form

$$E(x)=E_0q(x)e^{i\sigma(x)}\ , \tag{5.5}$$

where $E_0$ is the amplitude of the incoming wave; $q$ and $\sigma$ are real functions of the space variable $x$ and are the amplitude and phase, respectively, of the envelope function. Inserting (5.5) into (5.3) and collecting the imaginary part, one obtains after integration the following expression of the phase:

$$\sigma(x)=\int\frac{A}{I(x)}dx+\sigma_0\ , \tag{5.6}$$

where $A$ and $\sigma_0$ are constants of integration and $I(x)=q^2(x)$. The integration of the real part of the equation resulting from the substitutions of (5.5) into (5.3) gives the cnoidal wave type equation for $I(x)$:

$$\left[\frac{dI}{dx}\right]^2+2\frac{Q_r}{P}E_0^2I^3+4\frac{\Omega}{P}I^2-4BI+4A^2=0\ , \tag{5.7}$$

where $B$ is the arbitrary constant of integration; $A$ and $B$ are given by

$$A=\mu_1 k_L I_L \ , \tag{5.8}$$

$$B=\frac{\nu_3}{4}I_L^2+\left[(\mu_2^2+A_0^2)+\frac{\Omega}{P}\right]I_L \ . \tag{5.9}$$

Two important cases can now be considered: $Q_r/P\geq 0$ and $Q_r/P\leq 0$. It is important to note that in the case of no long-range interaction and no competitive or cooperative effects between short-range interactions ($J_p=0$), one has only $Q_r/P\geq 0$ in the continuum medium approximation, since $Q_r$ and $P$ are always positive [30,9]. Because of the long-range interaction and the competitive or cooperative short-range interaction effect, one should have both cases (i.e., $Q_r/P\geq 0$ or $Q_r/P\leq 0$) in the continuum approximation, depending on the domain of possible values of the long-range parameter $r$. Defining

$$\nu_3=\frac{2Q_r}{P}E_0^2, \quad \nu_2=\frac{2\Omega}{E_0^2 Q_r}, \quad \nu_1=\frac{-2PB}{Q_r E_0^2}, \quad \nu_0=\frac{2PA^2}{Q_r E_0^2} \ , \tag{5.10}$$

Eq. (5.7) becomes

$$\frac{dI}{\sqrt{-\nu_3[I^3+\nu_2 I^2+\nu_1 I+\nu_0]}}=\pm dx \ . \tag{5.11}$$

From the boundary conditions, we know that $I_L$ is one of the three zeros of the denominator of the lefthand side of Eq. (5.11). The two others are given by

$$I_1=-\left[\frac{I_L}{2}+\frac{\Omega}{Q_r E_0^2}\right] -\left[\left[\frac{I_L}{2}+\frac{\Omega}{Q_r E_0^2}\right]^2+\frac{2A^2P}{E_0^2 I_L Q_r}\right]^{1/2} , \tag{5.12}$$

$$I_2=-\left[\frac{I_L}{2}+\frac{\Omega}{Q_r E_0^2}\right] +\left[\left[\frac{I_L}{2}+\frac{\Omega}{Q_r E_0^2}\right]^2+\frac{2A^2P}{E_0^2 I_L Q_r}\right]^{1/2} . \tag{5.13}$$

In general, the integration of (5.11) assumes that one be able to arrange the roots $I_L$, $I_1$, and $I_2$; this implies some relations between lattice and wave parameters that are not always analytically expressible. To solve this apparent problem, we compute $I_{\min}$, $I_{\text{int}}$, and $I_{\max}$ from the following relations:

$$I_{\min}=\min[I_1,I_2,I_L] \ , \tag{5.14}$$

$$I_{\max}=\max[I_1,I_2,I_L] \ , \tag{5.15}$$

$$I_{\text{int}}=(I_1+I_2+I_L)-(I_{\max}+I_{\min}) \ . \tag{5.16}$$

These relations assign to $I_{\min}$, $I_{\max}$, and $I_{\text{int}}$, one of the variables $I_L$, $I_1$, and $I_2$, so that one always has $I_{\min}<I_{\text{int}}<I_{\max}$.

### A. Case 1: $Q_r/P\geq 0$

The standing wave solution exists only if $I_{\text{int}}<I<I_{\max}$, according to the value of $\Omega$, $I_{\text{int}}$ or $I_{\max}$ can be identified to $I_L$ and the other to $I_2$. Equation (5.11) now takes the form

$$\frac{dI}{\sqrt{(I_{\max}-I)(I-I_{\text{int}})(I_{\min})}}=\pm\sqrt{\nu_3}dx \ ; \tag{5.17}$$

the solution of (5.17) is then [32]

$$I(x)=\frac{I_{\text{int}}-mI_{\min}\,\text{sn}^2\left[\left[\frac{Q_r E_0^2(I_{\max}-I_{\min})}{2P}\right]^{1/2}(x-L),\sqrt{m}\right]}{1-m\,\text{sn}^2\left[\left[\frac{Q_r E_0^2(I_{\max}-I_{\min})}{2P}\right]^{1/2}(x-L),\ \sqrt{m}\right]} , \tag{5.18}$$

with

$$m=\frac{I_{\max}-I_{\text{int}}}{I_{\max}-I_{\min}} \ . \tag{5.19}$$

### B. Case 2: $Q_r/P\leq 0$

The root $I_{\min}$ is always negative and the standing wave solution arises only if $I_{\min}<I\leq I_{\text{int}}$ or $I_{\max}\leq I$. In the first case, $I_{\text{int}}$ is identified with $I_L$. In the linear case approximation, and with the particular choice of $\Omega$, one could have $I_L\simeq 0$; thus, $I(x)$ becomes negative and the solution is unphysical since $I(x)$ is the wave intensity at point $x$. For this reason, the second condition is valid: $I_{\max}\leq I$. The solution is, however, given by

$$I(x)=\frac{I_{\text{int}}-mI_{\max}\,\text{sn}^2\left[\left[\frac{-Q_r E_0^2(I_{\max}-I_{\min})}{2P}\right]^{1/2}(x-L),\sqrt{m}\right]}{1-m\,\text{sn}^2\left[\left[\frac{-Q_r E_0^2(I_{\max}-I_{\min})}{2P}\right]^{1/2}(x-L),\sqrt{m}\right]} , \tag{5.20}$$

with

$$m=\frac{I_{\text{int}}-I_{\min}}{I_{\max}-I_{\min}} . \tag{5.21}$$

The envelope wavelength in the nonlinear medium deduced from (5.18) and (5.20) is

$$\lambda=\frac{4K(m)}{E_0\left[\frac{1}{2}\left|\frac{Q_r}{P}\right|(I_{\max}-I_{\min})\right]^{1/2}} , \tag{5.22}$$

where $K(m)$ is the complete elliptic integral of the first kind. Once the standing wave solutions are known, one can compute the transmissivity of the nonlinear system. Using the boundary condition at $x=0$ and the condition on the wave at the output of the medium ($x=L$), we can now numerically study the influence of the long-range interactions on the transmission properties of the system according to the procedure of Chen and Mills [35–37].

## VI. NUMERICAL RESULTS AND DISCUSSION

In the following, we consider incoming waves with angular frequency near the gap threshold. The carrier wave number is at the middle of the Brillouin zone. Therefore, the group velocity is $v_g=0$. The nonlinearity and dispersion coefficients, respectively, take the form

$$Q=\frac{\omega_0'}{2}\left(\tfrac{10}{3}\alpha^2-3\beta\right) , \tag{6.1}$$

$$P=\frac{c^2(r)-\omega_0'^2 f(r)}{2\omega_0'} . \tag{6.2}$$

It is now clear that the long- and short-range parameters only modify the dispersion in the long-wavelength approximation. The numerical values of parameters used for our figures are in normalized units.

### A. Long-range interaction effects on the resonance curves

One of the problems in numerical analysis is the choice of realistic parameters for modeling the physical situation. First, we have to choose the length ($L$) of our finite nonlinear medium. Because of the possible resonance at the maximum of transmission, one must take care of this choice. At the resonance, one or more complete periodic waves must be observed in the nonlinear finite medium. Let us consider the wavelength $\lambda$ of the standing wave defined by (5.22) for a given value of $r$. At the resonance, we have $L=N_{\text{mod}}\lambda$, where $N_{\text{mod}}$ is an integer number of the envelope wavelength in the nonlinear medium. As shown in Figs. 3(a) and 3(b), the wavelength $\lambda$ depends on the incoming wave amplitude ($E_0$). In Fig. 3(a) (i.e., for $r\leq 0.4$, $\phi_0=0.0$, and $J_p=0.1$), the maximum wavelength corresponds to the linear approximation of the nonlinear medium ($E_0\simeq 0$), and increases with the long-range parameter $r$. As $E_0$ increases, the envelope wavelength decreases corresponding to a probable compression of the standing wave. The same behavior is observed in Fig. 3(b) for $r\geq 0.6$ after the maximum wavelength ($\lambda_{\max}$),

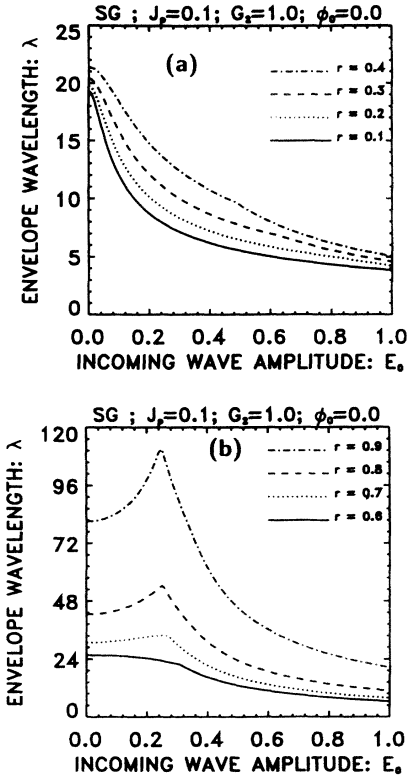


FIG. 3. Envelope wavelength $\lambda$ as a function of the incoming wave amplitude in the cooperative short-range interactions case ($J_p=0.1$ and $G_2=1.0$) and for an unperturbed sine-Gordon potential ($\phi_0=0$); (a) $r<0.5$, and (b) $r>0.5$.

which no longer corresponds to the linear case. Between the linear case ($E_0\simeq 0$) and the amplitude $E_{0m}$ corresponding to the maximum wavelength, we note the increase of the wavelength equivalent to a dilatation of the standing wave. If the length of the medium is chosen to be less than the maximum wavelength, for example, $L=15$, no complete standing wave will be observed in the nonlinear medium for $r=0.4$ if the maximum of transmission arises for $E_0<0.2$. Indeed, from Fig. 3(a), the wavelength is, in this case, greater than the length of the medium. The choice of $L$ for any given value of $E_0$ supposes that $\lambda$ is replaced by $\lambda_{\max}$, we have $L=N_{\text{mod}}\lambda_{\max}$. As $\lambda_{\max}$ increases with the long-range parameter, to study the transmission properties of our model, whatever $E_0$ and $r$, we must take $\lambda_{\max}$ corresponding to the greatest value of $r$.

### B. Long-range interaction effects on the transmission properties

The second step of our numerical studies is to study carefully what role parameters $r$ and $J_p$ play in the transmittance of the sine-Gordon system. The theory developed here is also valid for any potential, such as the $\Phi^4$ potential. The algorithm used here is that described by Chen and Mills [35–37]. Figure 4(a) is obtained for the incoming wave angular frequency $\omega=0.985$. The characteristic velocity $c_L$ and the harmonic constant of

interaction $G_2$ are chosen to be equal to 1.0. For $L=20$, we vary the incoming amplitude from approximately zero to 0.5. It follows that for a more extended range of interactions (i.e., increasing values of $r$), the number of the maximum of transmission decreases, the size of the hysteresis cycle is reduced, and the bistability progressively disappears. Figure 4(b) shows the effect of the long-range parameter on the envelope function. When $r$ increases, there is a progressive dilatation of the standing wave followed by a decrease of the maximal amplitude. These results correspond to the same characteristic parameters as in Fig. 4(a), namely, the unperturbed sine-Gordon system ($\phi_0=0.0$) and cooperative short-range interactions (i.e., $G_2=1.0$ and $J_p=0.1$). The behavior of the transmittance, as previously mentioned, depends on the length of the medium and on the long-range parameter. If this parameter is chosen such that the resonance curve corresponds to one of the curves of Fig. 3(b), the behavior of the transmittance will change because of the asymmetry shown by Fig. 3(b). First for $r \geq 0.7$ we must take higher values of the length for the reason previously mentioned. For $L=60$, and for the same characteristic parameters as in Fig. 4(a), the transmissivity is given in Fig. 5(a); we note that for $r=0.8$, the width of the bistability is more important than for $r=0.7$. Moreover, the appearance of the third maximum of transmission corresponds to the formation of a supplementary mode because of the conjugation of the compression and the resonance condition. In Fig. 5(b), we show envelope standing waves for (I) $r=0.7$, and for (II) and (III), $r=0.8$ for the same characteristic parameters as in Fig. 5(a). Curves (I) and (II) are obtained at the first maximum of transmission of curves in Fig. 5(a). Here again we note that, when $r$ increases, the width of the standing wave increases. Curve (III) of Fig. 5(b) corresponds to the third maximum of transmission of Fig. 5(a) obtained for $r=0.8$; it shows that there is

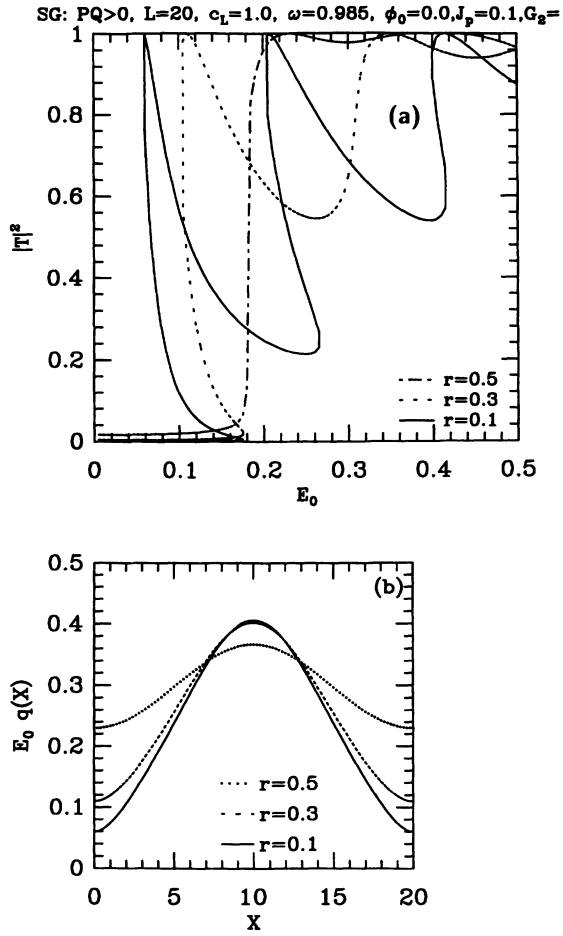


FIG. 4. (a) Transmissivity of the nonlinear medium as a function of the incoming wave amplitude $E_0$ for different values of $r$ (0.1, 0.3, 0.5). This corresponds to the case of cooperative short-range interactions ($J_p=0.1$, $G_2=1.0$) with $L=20$, $c_L=1.0$, $\omega=0.985$, and $\phi_0=0.0$ in normalized units. (b) Envelope amplitude in the nonlinear medium for different values of the long-range parameter. The different curves are obtained at the first maximum of transmission for each value of $r$.

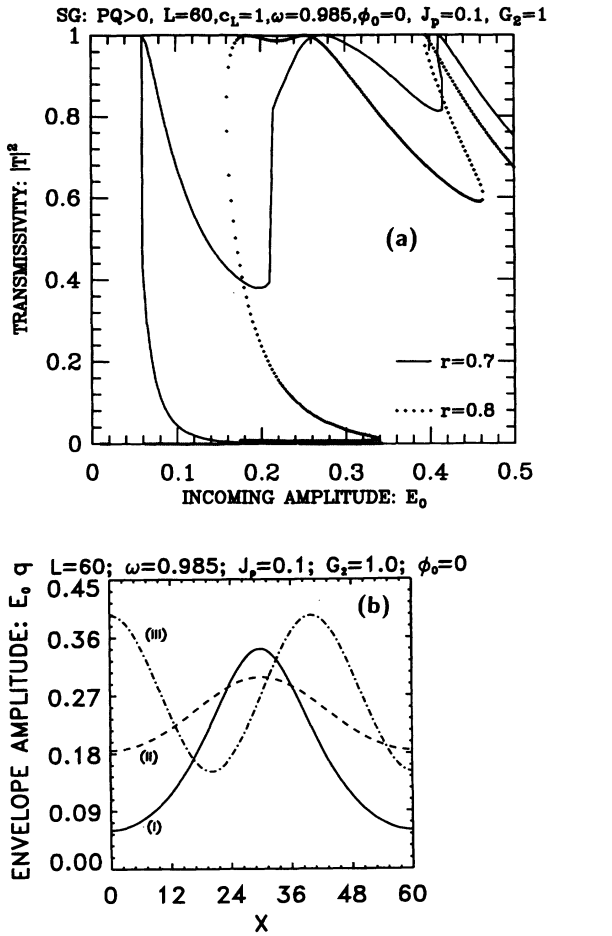


FIG. 5. (a) Nonlinear transmissivity versus the incoming wave amplitude for higher values of parameter $r$. Except for the value of the length $L=60$, the other characteristic parameters are the same as in Fig. 4(a). (b) Standing waves, relative to the finite envelope function for (I), $r=0.7$; and (II) and (III), $r=0.8$. Envelope functions (II) and (III), respectively, correspond to the first and third maximum of transmission of (a) ($r=0.8$). The variable $X$ is in units of the length scale $a$.

no integer number of envelope periods; therefore, there is no envelope resonance. The increase in the number of envelope modes is a manifestation of the nonlinear effect that shrinks the lower gap and allows the propagation of waves with forbidden frequencies.

Figure 6(a) shows the nonlinear transmissivity of the unperturbed sine-Gordon system allowing long-range interactions and competitive short-range interactions. As shown by Fig. 2, for $J_p=-0.1$ the hole solution is expected for $r>0.6$. We now look for the role of the long-range parameter when $PQ\leq 0$. Figure 6(a) is obtained for $L=90$ and $r=0.7$ and $r=0.8$, respectively; we note that the number of resonance states decreases when $r$ increases. Moreover, for a given value of $r$ the size of hysteresis increases from one cycle to the next. We have seen in Fig. 2 that in the case of competitive short-range interactions ($J_p=-0.1$) the coefficient $K=PQ$ is negative over a particular value ($r_c=0.6$) of $r$. As has been forseen by Remoissenet and Flytzanis, hole (or dark) type solutions are expected due to the long-range parameter. This theoretical result is confirmed in Fig. 6(b), where we can note the diminution of the number of envelope modes when the long-range interaction parameter increases. Simultaneously, the maximum amplitude increases.

### C. Short-range interaction effects on the transmission properties

We now look for the role played by the short-range interactions in the transmission properties of the system. Because $J_p$ and $r$ are independent variables, this will be done for $r=0$ and, in both cases, $J_p\geq 0$ and $J_p\leq 0$. In the cooperative short-range interaction case, Fig. 7(a), obtained for $L=16$ and $r=0$, shows that the incoming wave amplitude corresponding to the maximum of transmission and the threshold of bistability increases with the short-range parameter. Therefore, the size of the hysteresis cycle decreases. The stationary wave envelope obtained at the first maximum of transmission of each curve of Fig. 7(a) shows an increase of the amplitude

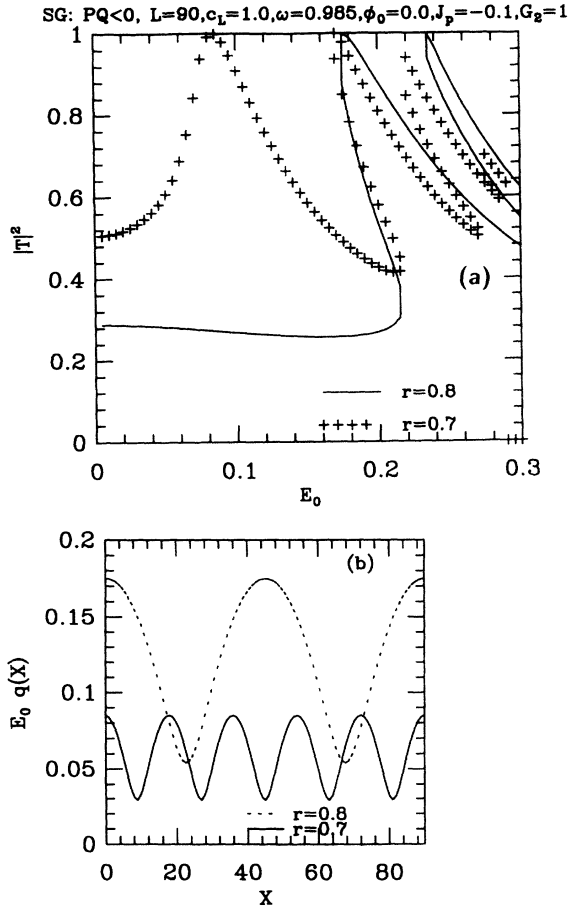


FIG. 6. (a) Effects of the long-range parameter on the transmissivity in the competitive short-range interactions case, and for $PQ<0$ with $L=90$; $J_p=-0.1$, $G_2=1.0$, $\omega=0.985$, and $c_L=1.0$. (b) Effects of the long-range parameter on envelope functions at the first maximum of transmission of curves in (a) relative to $r=0.7$ and $r=0.8$. These results are obtained for $L=90$, $\omega=0.985$, $J_p=-0.1$, $G_2=1.0$, and $\phi_0=0.0$.

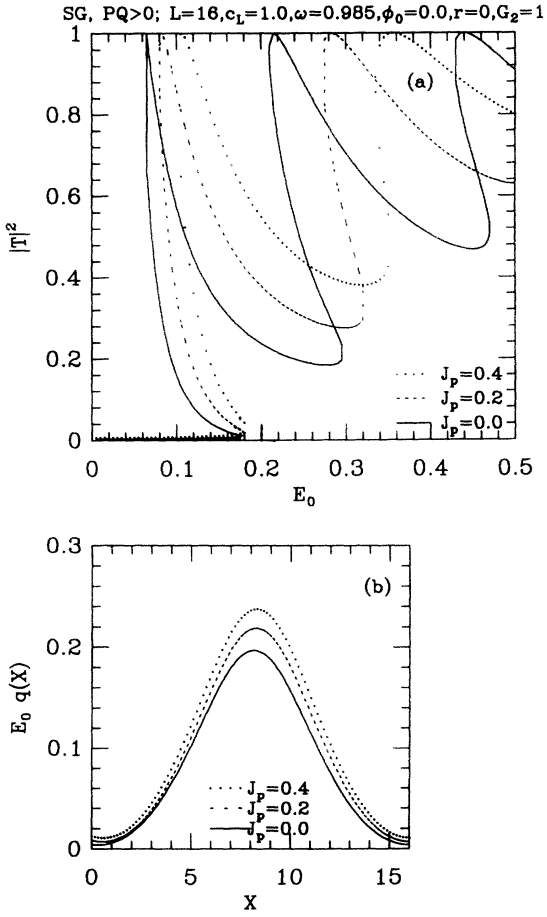


FIG. 7. (a) Cooperative effects of the short-range interactions on the transmissivity for $L=16$; $J_p=0.0,0.2,0.4$; $G_2=1.0$; $\omega=0.985$; and $c_L=1.0$. (b) Cooperative effects of the short-range parameter on envelope functions at the first maximum states of transmission. These results are obtained for $L=16$, $\omega=0.985$, $J_p=0.0,0.2,0.4$, $G_2=1.0$, and $\phi_0=0.0$.

and a progressive dilatation as $J_p$ increases, Fig. 7(b).

When short-range interactions are competitive, Fig. 8(a) shows that there is a diminution of the bistability threshold amplitude as $|J_p|$ increases. As a result, there is an extension of the hysteresis cycle that yields the multistability of the system transmission. Consequently, in the competitive short-range interactions, the system can switch from a bistable to a multistable state of transmission. As shown in Fig. 8(b), the envelope function in this case contrasts with that of the cooperative case: compression of the envelope, diminution and stretching of amplitude when $|J_p|$ increases.

### D. Limits of $r$ and $J_p$

Previous numerical studies show the effects of short- and long-range interactions on the nonlinear response of an excited finite system. A question remains unsolved: What are the limits of parameters $r$ and $J_p$ over which the nonlinear response of the system is unphysical? Because the system must be resonant [i.e., $I(0)=I(L)$]at

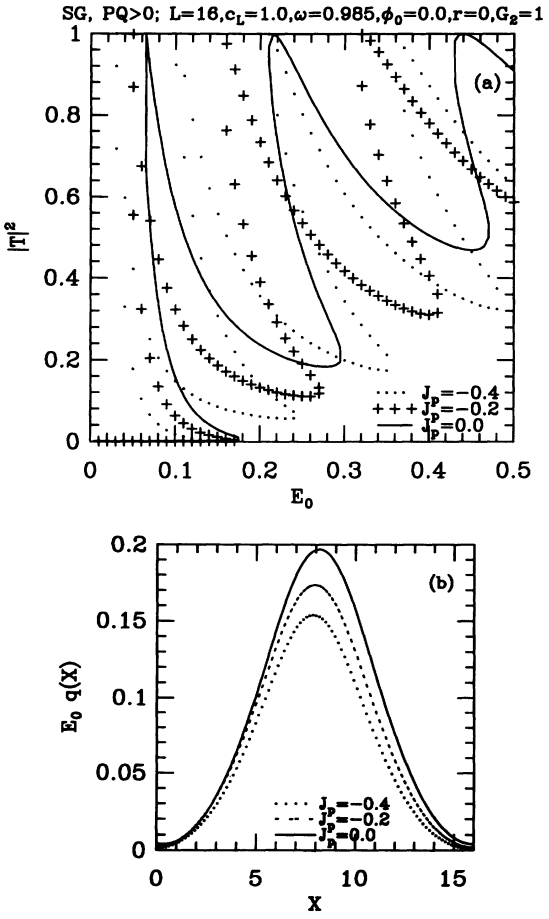


FIG. 8. (a) Competitive effects of the short-range interactions on the transmissivity for $L=16$, $J_p=0.0, -0.2, -0.4$, $G_2=1.0$, $\omega=0.985$, and $c_L=1.0$. (b) Competitive effects of the short-range parameter on envelope functions at the first maximum state of transmission. These results are obtained for the same characteristic parameters as in (a).

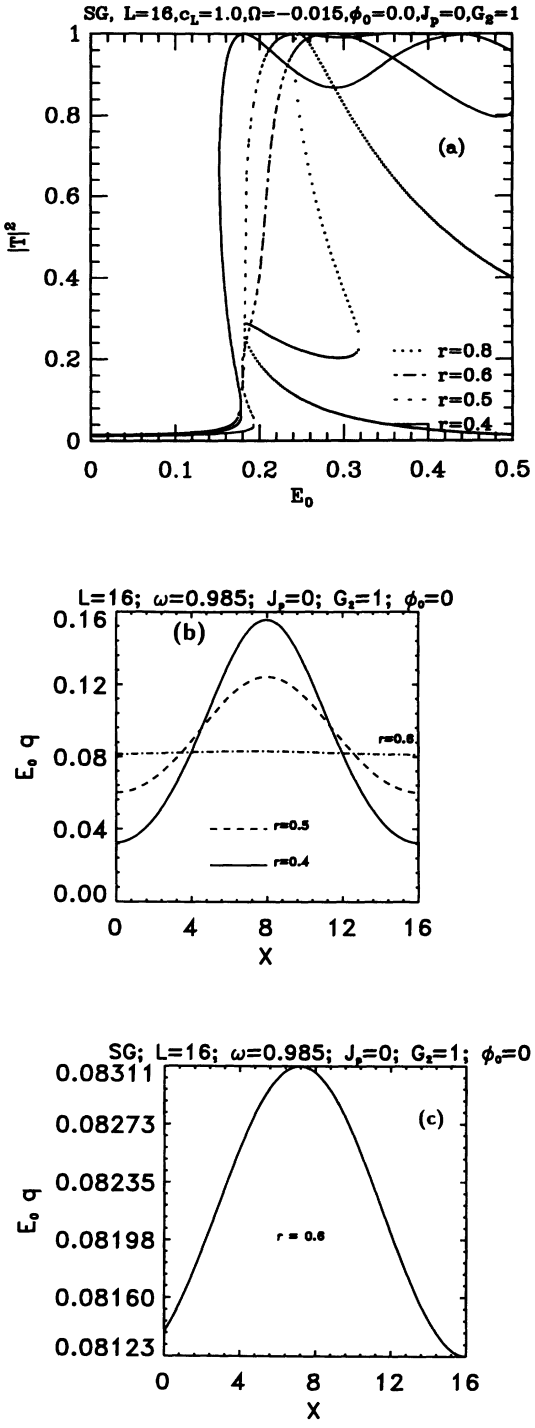


FIG. 9. (a) Illustration of the limiting values of the long-range parameter. Effects of the long-range interactions ($r=0.4$, $r=0.5$, $r=0.6$, $r=0.8$) on the nonlinear transmissivity in the case of no cooperative or competitive short-range interactions ($J_p=0$) and for $L=16$, $c_L=1.0$, $\omega=0.985$, $G_2=1.0$. (b) and (c) illustrate the long-range interaction effects on the standing wave function, in the case of no short-range interaction. Figures are obtained for $r=0.4, 0.5, 0.6$, $L=16$; $\omega=0.985$; $G_2=1.0$; and for the unperturbed sine-Gordon system. (b) shows that when the long-range interaction increases, the amplitude decreases. (c) shows that there is no more resonance after a certain value $r_c$ of $r$: $0.5<r_c<0.6$.

the maximum of transmission, the resonance condition will be taken as the basic criterion of our present investigation. Let us consider Fig. 9(a), corresponding to the transmission curves for $L=16$, $J_p=0$, and $r=0.4,0.5,0.6,0.8$. We note the tendency and the formation of a small hysteresis cycle, respectively, for $r=0.6$ and $r=0.8$. In Fig. 9(b), relative to stationary waves at the first maximum of transmission, we note that for $r=0.6$ and $r=0.8$, the envelope amplitude is very low. A zoom of this envelope as shown in Fig. 9(c) shows that there is no resonance in contrast to the expecting results. For $r=0.5$ and $r=0.6$, there is resonance within the system. The irregular behavior mentioned above, coming from the modulation of the long-range parameter, means that there is a critical value $r_c$ of $r$ over which there is no resonance. For values chosen in the present analysis, we have $0.5<r_c<0.6$. The exact value can be

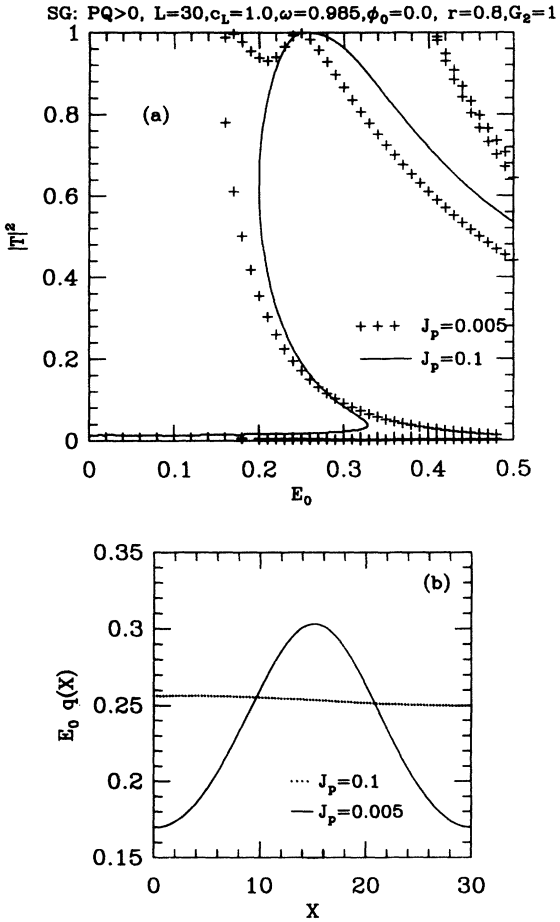


FIG. 10. (a) Effects of the short-range parameter $J_p$ on the transmittance of the unperturbed sine-Gordon system. Curves are obtained for $r=0.8$, $L=30$, $G_2=1.0$, $\omega=0.985$, and $c_L=1.0$. (b) Standing wave in the unperturbed sine-Gordon system for different values of the short-range parameter $J_p$ and for $r=0.8$ at the maximum of transmission. The other values used here are $L=30$, $\omega=0.985$, and $G_2=1.0$. There is no resonance for $J_p=0.1$ and the corresponding amplitude is very low. As seen previously, this shows that there is a limit $J_{pc}$ of $J_p$ for given values of $r$ and $L$.

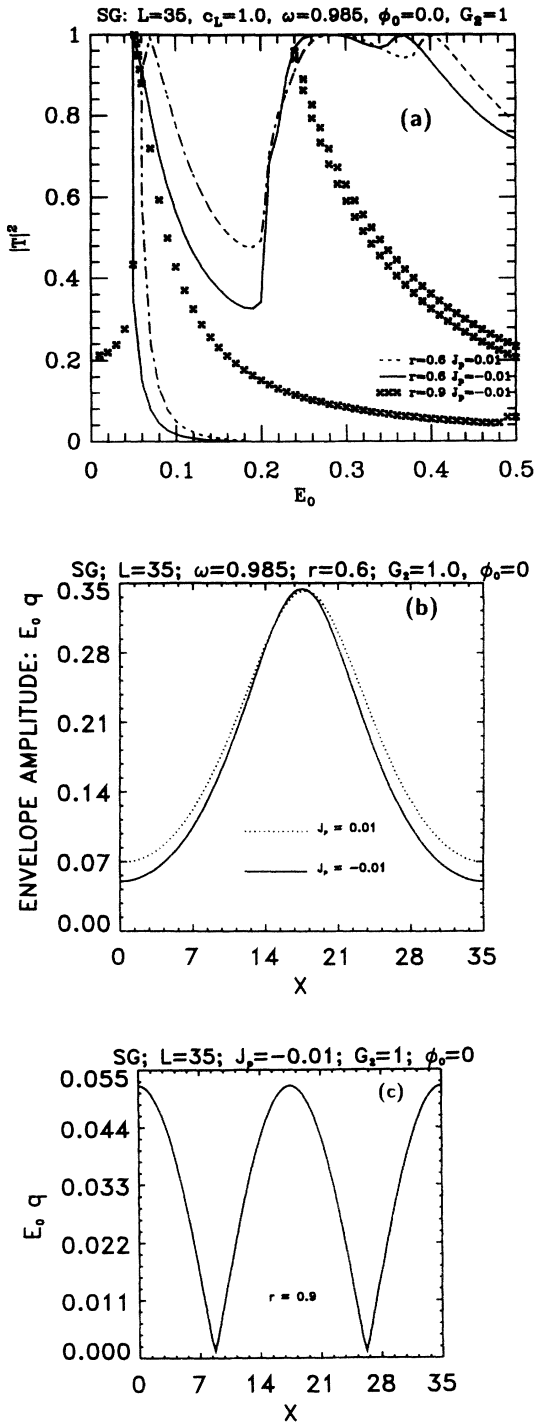


FIG. 11. (a) Comparison of the cooperative ($J_p=0.01$) and competitive ($J_p=-0.01$) effects on the nonlinear transmittance for $r=0.6$. The curves corresponding to $r=0.6$ and $r=0.9$, both for $J_p=-0.01$, show the effects of the long-range interactions on the nonlinear transmissivity for competitive effects with $L=35$, $c_L=1.0$, $\omega=0.985$, and $G_2=1.0$. (b) Comparison of the cooperative ($J_p=0.01$) and competitive ($J_p=-0.01$) short-range interactions effects on the standing wave function obtained for $r=0.6$, $L=35$, $\omega=0.985$, $G_2=1.0$ and for an unperturbed sine-Gordon system. (c) is the standing wave of a "dark" type for competitive short-range interactions ($J_p=-0.01$) and $r=0.9$. The other parameters are the same as in (a).

obtained by solving $L=N_{\text{mod}}\lambda$ according to the variable $r$, where $N_{\text{mod}}$ is the number of envelope periods in the system and $\lambda$ the wave number of the stationary elliptic wave. This limiting value of $r$ is a function of the length and the short-range interactions parameter.

We now look for the role played by the short-range parameter $J_p$ on the nonlinear transmission of the system. For this purpose, we choose $L=30$ and $r=0.8$; $c_L$ and $G_2$ remain the same as in the previous cases. Thus Fig. 10(a) shows that when $J_p$ increases, the number $N_r$ of maximum states of transmission decreases ($N_r=3$ for $J_p=0.0005$ against $N_r=1$ for $J_p=0.1$). The threshold $E_{0s}$ of bistability occurs for greater incident energy when $J_p$ decreases (for $J_p=0.0005$ and for $J_p=0.1$). Consequently, the memory of the systems due to hysteresis is less reliable as $J_p$ increases. Envelope functions presented in Fig. 10(b) are relative to the first maximum of each of the transmission curves presented. The role of $J_p$ is shown in Fig. 10(a). We note that for fixed values of $L$ and $r$, at the maximum of transmission, we do not have a complete standing wave (i.e., a wave extended on its entire period) for $J_p=0.1$. By decreasing the value of $J_p$ ($J_p=0.0005$), one period of a standing wave is obtained at the resonance. If $J_p$ is fixed at 0.1, resonance curves in Fig. 3(b) show that for $r=0.8$, we should increase the length ($L$) for 30 to 60 before obtaining a complete standing wave. Consequently, decreasing the value of $J_p$ for fixed values of $L$ and $r$ is almost equivalent to increasing $L$ for fixed values of $J_p$ and $r$.

### E. Coexistence of envelope and dark solutions

In Fig. 11(a), we compare the competitive and cooperative effects on the transmission coefficient for $L=35$; $c_L$, $\omega$, $G_2$, and $\phi_0$ are the same as in the previous case. For $r=0.6$, we note that the threshold of bistability does not significantly depend on the sign of $J_p$ (cooperative or competitive). The maximum of transmission is obtained for greater values of incident energy in the cooperative short-range interaction case. In the competitive case, when $r$ increases from 0.6 to 0.9, the size of the hysteresis cycle decreases, for $E_0 \geq 0.24$, we note the appearance of the second bistability for $r=0.9$, while that corresponding to $r=0.6$ disappears. In Fig. 11(b), we compare the role of cooperative and competitive short-range interactions on the envelope function. We note a compression of the envelope standing wave in the case of competitive interactions. When we increase the long-range parameter to $r=0.9$, there is a complete change of behavior of the solution since $PQ$ is negative. Instead of the envelope function, a "dark" type solution is obtained in Fig. 11(c). The number of modes increase for a low amplitude, compared to the case $r=0.6$ for the same value of $J_p$ (i.e., $J_p=-0.01$).

## VII. CONCLUSION

As forseen by Ishimori, using the Lennard-Jones coupling potential, and by Remoissenet and Flytzanis in the Kac-Baker-type long-range potential, we have shown that the long-range parameter plays a role only in the dispersion property of nonlinear systems in the long-wavelength approximation. In the competitive short-range interactions case, and for $r \to 1$, the threshold of the gap corresponds to an angular frequency $\omega_m \neq \omega_0'$ that increases (up to $\omega_0'$) when the short-range coupling parameter $J_p$ decreases. For a quartic anharmonic sine-Gordon system with competitive short-range interactions, envelope and hole standing waves can coexist. The existence domain of each solution depends on the short-range parameter $J_p$. The numerical study of the nonlinear response of the system discloses the fact that the envelope resonance is linked to the maximum state of transmissivity and to the length of the system, which must be greater than the envelope wavelength relative to the corresponding incoming wave amplitude. Even if a given value of the length of the nonlinear system does not give rise to the physical envelope resonance, one can nevertheless reach this state by decreasing progressively the value of the short-range coupling parameter. In the cooperative short-range interaction case, when the intensity of long-range interactions increases (i.e., increasing values of parameter $r$), the size of the hysteresis cycle decreases and the bistability tends to disappear. Simultaneously, the width of the standing wave decreases. It is found that in a finite system, increasing the value of length ($L$) for a fixed value of $J_p$ or decreasing the value of $J_p$ for a fixed value of $L$ allows us to have elementary excitations even for a higher interaction range ($r \to 0.8; 0.9$). For fixed values of $L$ and $J_p$, there is a limit $r_c$ of $r$ over which no elementary excitation is observed. As examples of applications, we have based our numerical studies on a sine-Gordon system, but it can also be applied to other types of systems such as the $\Phi^4$ system, double sine-Gordon system, etc. Finally, we hope that the general approach of our studies provides applications in many fields of physics, particularly in optics and in solid state physics.

[1] D. L. Mills and S. E. Trullinger, Phys. Rev. B **36**, 947 (1987).
[2] C. Martijn de Sterke and J. E. Sipe, Phys. Rev. A **38**, 5149 (1988).
[3] S. Dutta Gupta, J. Opt. Soc. Am. B **6**, 1927 (1989).
[4] L. Kahn, N. S. Almeida, and D. L. Mills, Phys. Rev. B **37**, 8072 (1988).
[5] D. Barday and M. Remoissenet, Phys. Rev. B **41**, 10 387 (1990).
[6] U. Trutschel and F. Lederer, J. Opt. Soc. Am. B **5**, 2530 (1988).
[7] Kevin L. Stokes and Ashok Puri, Opt. Lett. **15**, 1986 (1990).
[8] Subhasish Dutta Gupta and Deb Shankar Ray, Phys. Rev. B **38**, 3628 (1988).
[9] J. M. Bilbault, C. Tatuam Kamga, and M. Remoissenet,

Phys. Rev. B **47**, 5748 (1993).
[10] J. Frenkel and T. Kontorova, Zh. Eksp. Teor. Fiz. **8**, 89 (1938); [J. Phys. (Moscow) **1**, 137 (1939)].
[11] M. Toda, J. Phys. Soc. Jpn. **22**, 431 (1967).
[12] V. L. Pokrovsky and A. Virostek, J. Phys. C **16**, 4513 (1983).
[13] O. M. Braun, Yu. S. Kivshar, and I. I. Zelenskaya, Phys. Rev. B **41**, 7118 (1990).
[14] Y. Ishimori, Prog. Theor. Phys. **68**, 402 (1982).
[15] George A. Baker, Jr., Phys. Rev. **122**, 1477 (1961).
[16] M. Kac and E. Helfand, J. Math. Phys. **4**, 1078 (1973).
[17] K. S. Viswanathan and D. H. Meyer, Physica (Utrecht) A **89**, 97 (1977).
[18] S. K. Sarker and J. A. Krumhansl, Phys. Rev. B **23**, 2374 (1981).
[19] P. Woafo, T. C. Kofané, and A. S. Bokosah, J. Phys. Condens. Matter **3**, 2279 (1991).
[20] P. Woafo, T. C. Kofané, and A. S. Bokosah, J. Phys. Condens. Matter **4**, 3389 (1992).
[21] P. Woafo, T. C. Kofané, and A. S. Bokosah, Phys. Rev. B **48**, 10 153 (1993).
[22] M. Remoissenet and N. Flytzanis, J. Phys. C **18**, 1573 (1985).
[23] C. Tchawa, T. C. Kofané, and A. S. Bokosah, J. Phys. A **26**, 6477 (1993).
[24] M. Rodrigo Ferrer, Phys. Rev. B **40**, 11 007 (1989).
[25] P. Woafo, J. R. Kenne, and T. C. Kofané, J. Phys. Condens. Matter **5**, L123 (1993).
[26] J. R. Kene, P. Woafo, and T. C. Kofané, J. Phys. Condensed Matter (to be published).
[27] M. Croitoru, J. Phys. A **22**, 845 (1989).
[28] P. Woafo and T. C. Kofané, Solid State Commun. **87**, 921 (1993).
[29] A. M. Dikande and T. C. Kofané, Physica D (to be published).
[30] M. Remoissenet, Phys. Rev. B **33**, 2386 (1986).
[31] R. Knapp, G. Papanicolaou, and B. White, in *Disorder and Nonlinearity,* edited by A. R. Bishop, Springer Proceedings in Physics Vol. 39 (Springer, Berlin, 1989), pp. 2–26.
[32] P. F. Byrd, and Morris D. Friedman, *Handbook of Elliptic Integrals for Engineers and Scientists,* 2nd ed., revised (Springer-Verlag, Berlin, 1971).
[33] Akira Tsurui, Prog. Theor. Phys. **48**, 1196 (1972).
[34] N. Flytzanis, St Pnevmatikos, and M. Remoissenet, J. Phys. C **18**, 4603 (1985).
[35] Wei Chen and D. L. Mills, Phys. Rev. Lett. **58**, 160 (1987).
[36] Wei Chen and D. L. Mills, Phys. Rev. B **35**, 524 (1987).
[37] Wei Chen and D. L. Mills, Phys. Rev. B **36**, 6269 (1987).